MOLECULAR AND CELLULAR BIOLOGY, Nov. 2007, p. 7683–7692 Vol. 27, No. 21
0270-7306/07/$08.00+0 doi:10.1128/MCB.00577-07

Essential Role of Endothelial Smad4 in Vascular Remodeling and Integrity▽†

Yu Lan,[1] Bing Liu,[2] Huiyu Yao,[2] Fangfei Li,[1] Tujun Weng,[1] Guan Yang,[1] Wenlong Li,[1] Xuan Cheng,[1] Ning Mao,[2] and Xiao Yang[1]*

Genetic Laboratory of Development and Diseases, Institute of Biotechnology, Beijing 100071,[1] and Department of Cell Biology, Institute of Basic Medical Sciences, Beijing 100850,[2] People's Republic of China

Received 2 April 2007/Returned for modification 30 May 2007/Accepted 13 August 2007

New blood vessels are formed through the assembly or sprouting of endothelial cells (ECs) and become stabilized by the formation of perivascular matrix and the association with supporting mural cells. To investigate the role of endothelial Smad4 in vascular development, we deleted the *Smad4* gene specifically in ECs using the Cre-*Lox*P system. EC-specific *Smad4* mutant mice died at embryonic day 10.5 due to cardiovascular defects, including attenuated vessels sprouting and remodeling, collapsed dorsal aortas, enlarged hearts with reduced trabeculae, and failed endocardial cushion formation. Noticeably, Smad4-deficient ECs demonstrated an intrinsic defect in tube formation in vitro. Furthermore, the mutant vascular ECs dissociated away from the surrounding cells and suffered from impaired development of vascular smooth muscle cells. The disturbed vascular integrity and maturation was associated with aberrant expression of angiopoietins and a gap junction component, connexin43. Collectively, we have provided direct functional evidence that Smad4 activity in the developing ECs is essential for blood vessel remodeling, maturation, and integrity.

The cardiovascular system is the first organ to develop and become functional during embryogenesis (23). For vascular maturation and stabilization, endothelial cells (ECs) recruit various types of mural cells to envelope the inner endothelial monolayer (4). Several ligand-receptor systems have been implicated in regulating vascular formation, stabilization, remodeling, and functioning through the interaction between ECs and pericytes. Such signaling systems include angiopoietins (Angs) and their Tie receptors, platelet-derived growth factor B (PDGFB) and platelet-derived growth factor receptor β (PDGFR-β), and the transforming growth factor β (TGF-β) superfamily (4).

The TGF-β superfamily members transduce their signals through transmembranous receptors (TβR) and intracellular mediator Smads (43). TGF-β seems to regulate stabilization of vessels in multiple ways, including stimulating synthesis and deposition of extracellular matrix (ECM) components, inducing the differentiation of mesenchymal cells to mural cells, and regulating several cellular processes in both ECs and mural cells (16, 23). Genetic studies in human beings and mice have revealed pivotal roles of TGF-β signaling during angiogenesis (7, 18, 22, 24, 29, 31, 32, 34, 48). Although mice deficient for various TGF-β signaling components present an embryonic lethality due to angiogenetic defects, there exist certain discrepancies among the vascular phenotypes (7, 22, 24, 31, 32, 34, 48). It is presumably due to the different expression pattern and the largely distinct target genes of the signaling components (12, 33, 47).

Smad4 is a central mediator of TGF-β signaling. Clinically, mutation in *Smad4* causes a syndrome consisting of both juvenile polyposis and hereditary hemorrhagic telangiectasia phenotypes (11), emphasizing its pathological involvement in human vascular disorders. Furthermore, controlling an angiogenic switch, other than mediating TGF-β's antiproliferative responses, has been assumed for Smad4 to serve as an alternative mechanism of tumor suppression (37). These findings strongly suggest a crucial role for Smad4 signaling in adult angiogenesis. Nevertheless, the precise roles of Smad4 in embryonic angiogenesis, in particular that as the unique common Smad, how it balances the two distinct TβRI pathways in ECs (12, 23), is by far unknown.

To address definitively the role of endothelial Smad4 in vascular development, we deleted the *Smad4* gene specifically in ECs by using the Cre-*Lox*P system with a mouse strain that specifically expressed Cre recombinase in ECs under the control of *Tie2* promoter (26). Here we show that the deletion of Smad4 in ECs results in embryonic lethality by embryonic day 10.5 (E10.5) due to cardiovascular defects, including attenuated vascular sprouting, ruptured blood vessels, and defective myocardial, as well as endocardial cushion development. Notably, Smad4-deficient ECs demonstrate an intrinsic defect in tube formation in vitro. In addition, our data also suggest that Ang2 and a gap junction component, connexin43 (Cx43), may serve as candidate targets of endothelial Smad4 signaling for maintaining intercellular interaction between ECs and surrounding cells, and therefore protecting vascular integrity and maturation.

MATERIALS AND METHODS

Mouse strains. Mice carrying conditional *Smad4* alleles (*Smad4*$^{Co/Co}$) (49) were bred with *Tie2-Cre* transgenic mice, in which expression of Cre recombinase is driven by promoter and enhancer of *Tie2* (26). To visualize cells with recombined alleles, mice bearing *Tie2-Cre* transgene were crossed with ROSA26 re-

* Corresponding author. Mailing address: Institute of Biotechnology, 20 Dongdajie, Beijing 100071, People's Republic of China. Phone and fax: 86-10-63895937. E-mail: yangx@nic.bmi.ac.cn.

† Supplemental material for this article may be found at http://mcb.asm.org/.

▽ Published ahead of print on 27 August 2007.

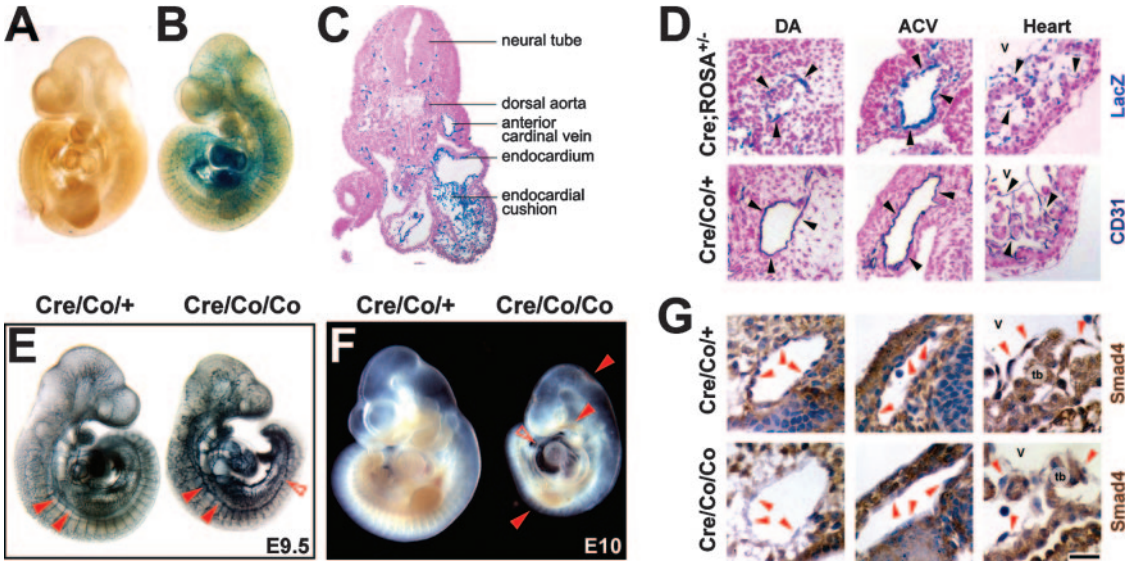

FIG. 1. EC-specific deletion of *Smad4* gene results in embryonic lethality at E10.5. (A and B) Whole-mount LacZ-stained *ROSA26* transgenic embryos without (A) or with (B) *Tie2-Cre* transgene at E9.5. (C) Cross section of LacZ-stained *Tie2-Cre; ROSA26* double-transgenic mice at E9.5 shows blue-stained ECs. (D) Cross sections of LacZ-stained *Tie2-Cre; ROSA26* double transgenic mice and whole-mount CD31-stained $Smad4^{Co/+}$; *Tie2-Cre* embryos at E9.5. The expression pattern between both stainings and the intensity of LacZ positive signals among the DAs, ACVs, and hearts are comparable. Arrowheads denote representative positive signals in the ECs. (E) Whole-mount CD31 immunostaining of E9.5 embryos shows apparent presence of major blood vessels in the mutant ones. Arrowheads denote DAs that are significantly narrowed in the mutant embryos. An open arrowhead denotes a discontinuity in the mutant DAs. (F) A whole-mount view shows growth retardation and cardiovascular defects in $Smad4^{Co/Co}$; *Tie2-Cre* embryos at E10. Arrowheads point to focal hemorrhage; the open arrowhead points to enlarged edematous pericardium. (G) Smad4 immunostaining of E9.5 embryos shows absent expression in the vascular ECs and endocardium of the mutant embryos. Arrowheads denote representative ECs. V, ventricles; tb, trabeculae. Scale bar: 500 μm (A, B, and E), 125 μm (C), 45 μm (D), 700 μm (F), or 25 μm (G).

porter mice (39). Animals were handled in accordance with institutional guidelines. Littermate embryos were used in all experiments.

Whole-mount embryo immunostaining and LacZ staining. Whole-mount embryo immunostaining with anti-CD31 antibody (BD Pharmingen) and whole-mount LacZ staining were performed as described previously (26, 34). The whole-mount preparations were documented by using a dissecting microscope (SMZ1500; Nikon, Tokyo, Japan) with a digital camera (RT color; SPOT; Diagnostic Instruments, Sterling Heights, MI). Stained tissues were further paraffin embedded, and sections were counterstained with nuclear fast red.

Histology, immunohistology, and electron microscopy. Mouse tissues were fixed in Bouin's fixative, embedded in paraffin, sectioned at 5 μm, and stained with hematoxylin and eosin by standard methods. Immunohistology was also performed by standard procedures. The primary antibodies used were as follows: anti-Smad4 (Santa Cruz), anti-α-smooth muscle actin (anti-α-SMA; Sigma), anti-CD31, antilaminin (Zymed), and anti-Cx43 (Sigma). A Nikon (Tokyo, Japan) E600 microscope with a digital camera (RT color; SPOT; Diagnostic Instruments) was used for documentation. Nikon 10×/0.30-numerical aperture (NA), 20×/0.50-NA or 40×/0.75-NA Plan Fluor objective lenses were applied. Electron microscopic analysis was performed as described previously (40). Ultrathin sections were stained in uranyl acetate and lead citrate and examined by using a Philips EM400 electron microscope.

Flow cytometry, isolation of embryonic ECs, and cell culture. E9.5 embryonic cells were harvested by trypsin-EDTA digestion. For flow cytometric analysis, cells were stained with phycoerythrin-conjugated isotype or phycoerythrin-conjugated anti-mouse Tie2 antibodies (eBioscience) according to the manufacturer's instructions. For Tie2-positive cells sorting, the dissociated cells were plated on mouse embryonic fibroblasts in culture medium described previously (14). After three passages of expansion on mouse embryonic fibroblasts, ECs were isolated by using magnetic bead (MACS Anti-Biotin MicroBeads; Miltenyi Biotec) purification with biotin-conjugated anti-mouse Tie2 antibody (eBioscience) according to the manufacturer's instructions. Selective transforming of ECs with a retrovirus expressing the polyoma middle T (PmT) oncogene and maintaining of the EC culture were performed as described previously (22). PmT-transformed ECs were incubated in the presence or absence of 10 ng of TGF-β1 (R&D Systems)/ml for 20 h prior to harvest if needed.

DiI-Ac-LDL incorporation and immunofluorescence staining. The adherent cells of the cultures were incubated with 10 μg of DiI-Ac-LDL (1,19-dioctadecyl-3,3,39,39-tetoramethylindo-carbocyanine perchlorate acetylated low-density lipoprotein; Biomedical Technologies, Inc.)/ml for 4 h at 37°C, fixed with 4% paraformaldehyde–phosphate-buffered saline, and counterstained with DAPI (4′,6′-diamidino-2-phenylindole). Immunofluorescence labeling of VE-cadherin (BD Pharmingen) and Cx43 was performed as described previously (20). Phase-contrast and fluorescence images were collected by using a Nikon TE2000-U inverted microscope with Nikon 4×/0.13 NA, 10×/0.30 NA, or 20×/0.45 NA Plan Fluor objective lenses. Images were acquired by using a digital camera (Cool SNAP 5.0; Roper Scientific, Tucson, AZ). Adobe Photoshop 7 software (Adobe Systems, Munich, Germany) was used for all of the figure preparation.

In vitro tube formation assay. After cultured for another 5 days, sorted embryonic ECs were collected by trypsin-EDTA digestion, replated to 48-well plates precoated with a thin layer of Matrigel (BD Biosciences), and allowed to form tube-like structures. ECs were quantified by counting branches from each EC and the length of the tube formed at 8 h. Measurement was performed in four independent fields, and the experiment was repeated three times. Statistical analysis was applied by using two-tailed Student *t* test.

Reporter gene assay. PmT-transformed ECs were seeded in 24-well plates and transfected with different reporter constructs with Lipofectamine (Invitrogen) according to the manufacturer's instructions. After 24 h, the cells were incubated in the presence or absence of BMP2 (R&D Systems) or TGF-β1 for another 16 h prior to harvest for luciferase assay. Each experiment was performed with triplicate samples and repeated three times.

RT-PCR and real-time PCR. For reverse transcription-PCR (RT-PCR) analysis, total RNA from E9.5 embryos or isolated embryonic ECs was extracted by using TRIZOL reagent (Invitrogen) and reverse transcribed by using an mRNA selective PCR kit (TaKaRa). Sequences of specific primers and amplified product sizes are listed in Table S1 in the supplemental material. Quantitative real-time PCR analysis and related primers were as described previously (41).

Western blotting. The total proteins from E9.5 embryos or cultured PmT-transformed ECs were harvested. Portions (20 μg) of the proteins were subjected to sodium dodecyl sulfate–12% polyacrylamide gel electrophoresis. Immunoblot-

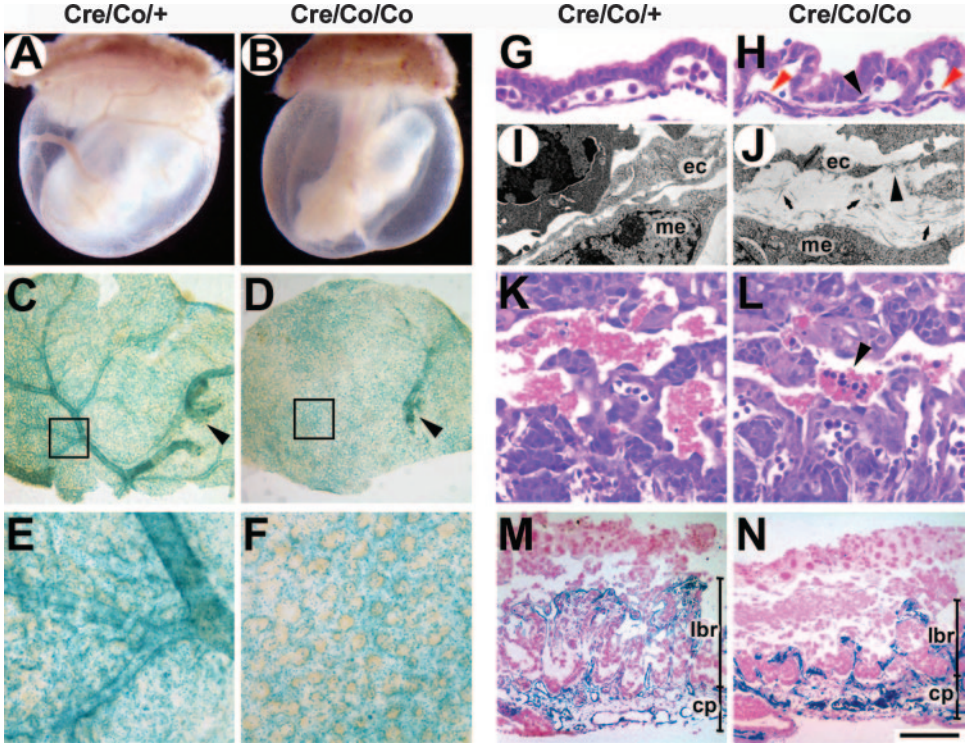

FIG. 2. Disturbed vascular remodeling in *Smad4*$^{Co/Co}$*; Tie2-Cre* YS and placentas. (A and B) Whole-mount view of E9.5 YS. (C and D) Whole-mount view of LacZ-stained YS of *Smad4*$^{Co/+}$*; Tie2-Cre* and *Smad4*$^{Co/Co}$*; Tie2-Cre* embryos carrying a *ROSA26* allele. Arrowheads denote the major vessels extended from embryos proper. (E and F) Higher magnifications of panels C and D, respectively. There is proper remodeling of vitelline vessels in control mice, which is absent in the mutants. (G and H) Hematoxylin-and-eosin-stained sections of E9.5 YS show EC layers of mutant YS dissociate from surrounding cells. Red arrowheads denote the ECs away from the subjacent mesothelial layer. A black arrowhead points to an EC detached from the endodermal layer. (I and J) Electron micrographs of E9.5 YS. Abnormal deposits of ECM (arrows) separate ECs from subjacent mesothelial cells in the mutant YS. An arrowhead denotes a discontinuity in the ECs. (K and L) Hematoxylin-and-eosin-stained placental sections at E9.5. Arrowhead shows leakage of embryonic nucleated erythrocytes in the maternal blood sinuses. (M and N) Histological sections of LacZ-stained placentas of *Smad4*$^{Co/+}$*; Tie2-Cre* and *Smad4*$^{Co/Co}$*; Tie2-Cre* embryos carrying a *ROSA26* allele at E10. The mutant placentas have a thinner labyrinth with fewer fetal vessels compared to the controls. ec, endothelial cells; me, mesothelial cells; lbr, labyrinth; cp, chorionic plate. Scale bar: 1,000 μm (A and B), 1,100 μm (C and D), 220 μm (E, F, M, and N), 43 μm (G and H), 2 μm (I and J), or 55 μm (K and L).

ting was performed with anti-Smad4, anti-Ang2 (Chemicon), anti-Cx43, and anti-actin (Sigma) according to the manufacturer's instructions.

RESULTS

EC specific deletion of *Smad4* gene resulted in embryonic lethality. We used the Cre-*Lox*P strategy with a *Tie2-Cre* transgenic mouse we have previously generated (26). Whole-mount LacZ staining for embryos proper at E9.5 of the *Tie2-Cre; ROSA26* double transgenic mice showed that blue-stained cells constituted the inner layer of the heart and all of the vessels throughout the cardiovascular system, whereas no LacZ staining was detected in mice without *Tie2-Cre* transgene (Fig. 1A to C). The same staining pattern between LacZ and CD31, as well as the equivalent intensity of LacZ-positive signals in dorsal aortas (DAs), anterior cardinal veins (ACV), and hearts, confirmed the specific and uniform expression of Cre recombinase in virtually all of the ECs during early vascular development (Fig. 1D).

To develop an endothelium-specific *Smad4* knockout mouse, we bred a mouse strain containing *Smad4* conditional alleles (*Smad4*$^{Co/Co}$) (49) with the *Tie2-Cre* transgenic mice. The acquired *Smad4*$^{Co/+}$*; Tie2-Cre* mice were further mated to *Smad4*$^{Co/Co}$ mice to generate *Smad4*$^{Co/Co}$*; Tie2-Cre* mice. A total of 72 offspring (from 13 litters) were genotyped, and no *Smad4*$^{Co/Co}$*; Tie2-Cre* pups were found, demonstrating the embryonic lethality.

Subsequently, a total of 56 litters were examined between E8.5 and E12.5. Conditional knockout embryos were morphologically indistinguishable from their wild-type littermates at E9 but were readily identifiable at E9.5 by their avascular yolk sacs (YS) and smaller body size (Fig. 1E and 2B). Visualization of endothelial networks with whole-mount CD31 staining demonstrated the presence of major blood vessels in the mutant embryos, but the DAs in the trunk manifested a decreased diameter and were even discontinuous (Fig. 1E). At E10, *Smad4*$^{Co/Co}$*; Tie2-Cre* embryos showed severe growth retardation, focal hemorrhage, and enlarged pericardium (Fig. 1F) but still had beating hearts. They died at E10.5, displaying severe distortion and diminished vasculature, and were resorbed by E11 (data not shown). Immunohistochemical staining verified the efficient disruption of *Smad4* gene in the endocardium and ECs of all of the vessels, including aortas and veins (Fig. 1G).

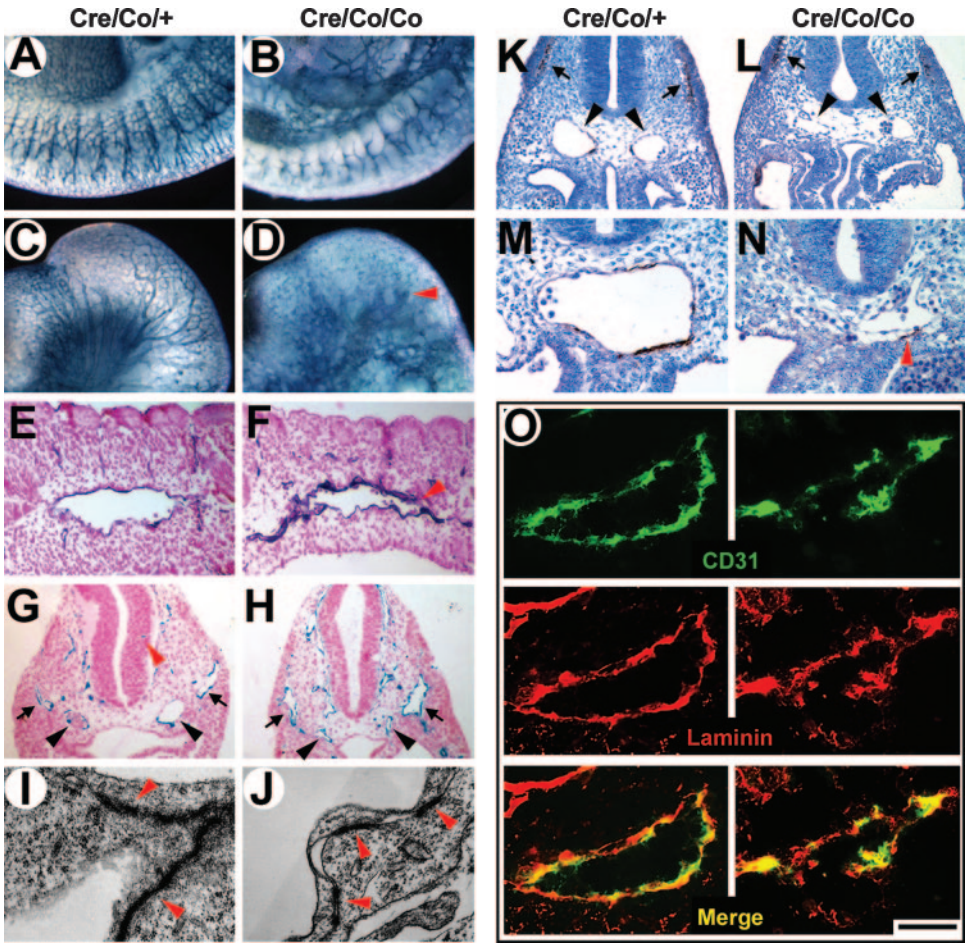

FIG. 3. Abnormal vasculature and impaired VSMC/pericytes development in *Smad4*$^{Co/Co}$*; Tie2-Cre* embryos. (A to D) Whole-mount CD31 immunostaining of E10 embryos. The mutant embryos show a coarse vascular plexus and significantly reduced capillary vessels in the intersomitic (A and B) and head region (C and D). Arrowhead indicates blind ending vessels. (E and F) Histological sections of whole-mount CD31-stained E9.5 embryos. The mutant embryos manifest an irregularly narrowed DA lumen. An arrowhead denotes the rupture of DA. (G and H) Histological sections of LacZ-stained *Smad4*$^{Co/+}$*; Tie2-Cre* and *Smad4*$^{Co/Co}$*; Tie2-Cre* embryos carrying a *ROSA26* allele at E9.5. The mutant embryos show remarkably narrowed DAs (black arrowheads) and moderately dilated ACV (arrows). A red arrowhead denotes vessels sprouted into the neural tissue of the control mice, which is absent in the mutant embryos. (I and J) Electron micrographs of inter-endothelial junctions (arrowheads) at E9.5 show a reduced junctional overlapping in the mutant vascular ECs. (K to N) α-SMA immunostaining of E9.5 embryos. Dramatically reduced expression around DAs in the mutant embryos is in contrast to the controls in which perivascular walls are lined with α-SMA-positive VSMC/pericytes. Black arrowheads denote DAs, and arrows denote the comparable α-SMA expression at the somites. A red arrowhead denotes the only α-SMA-positive cell in the field but detached from the EC layer. (O) Laminin immunofluorescence staining of E9.5 DAs shows a comparable expression level but abnormal deposition around the DAs of the mutant embryos. Scale bar: 420 μm (A through D), 100 μm (E and F), 150 μm (G, H, K, and L), 500 nm (I and J), 75 μm (M and N), or 40 μm (O).

In the present study, the *Smad4*$^{Co/+}$*; Tie2-Cre* mice were used as controls because they appeared no different from *Smad4*$^{Co/Co}$, *Smad4*$^{Co/+}$, or wild-type mice.

Disturbed vascular remodeling in *Smad4*$^{Co/Co}$*; Tie2-Cre* YS and placentas. Whereas control embryos had a well-perfused and hierarchically structured YS vasculature with branching vitelline vessels at E9.5 (Fig. 2A, C, and E), *Smad4*$^{Co/Co}$*; Tie2-Cre* embryos exhibited hemorrhage in the YS without obvious vascular structures (Fig. 2B). The mutant YS plexus failed to generate distinct vitelline vessels to connect with those vessels extended from embryos proper, remaining a meshwork of interconnected and homogeneously oversized EC-lined tubes (Fig. 2D and F). Histologically, the EC layer of mutant YS displayed ill-defined contact with mesothelial and endodermal layers by E9.5 (Fig. 2G and H). Electron microscopic evaluation confirmed the detachment and revealed abnormal deposits of the ECM in gaps separating mesothelium from the endothelium in *Smad4* mutants (Fig. 2I and J).

Vascular defects were also observed in the placental labyrinth. At E9.5, the labyrinth region in the control placentas contained a network of extra-embryonic capillaries interspersed with maternal sinuses, where two kinds of erythrocytes were separated (Fig. 2K). Of note, in the mutant labyrinth, clusters of embryonic nucleated erythrocytes were detected in the maternal sinuses, indicating the impaired integrity of mutant vessels (Fig. 2L). By E10, although the chorionic plate and trophoblast giant cells appeared normal, the labyrinth layer was reduced in thickness and less vascularized, as shown by

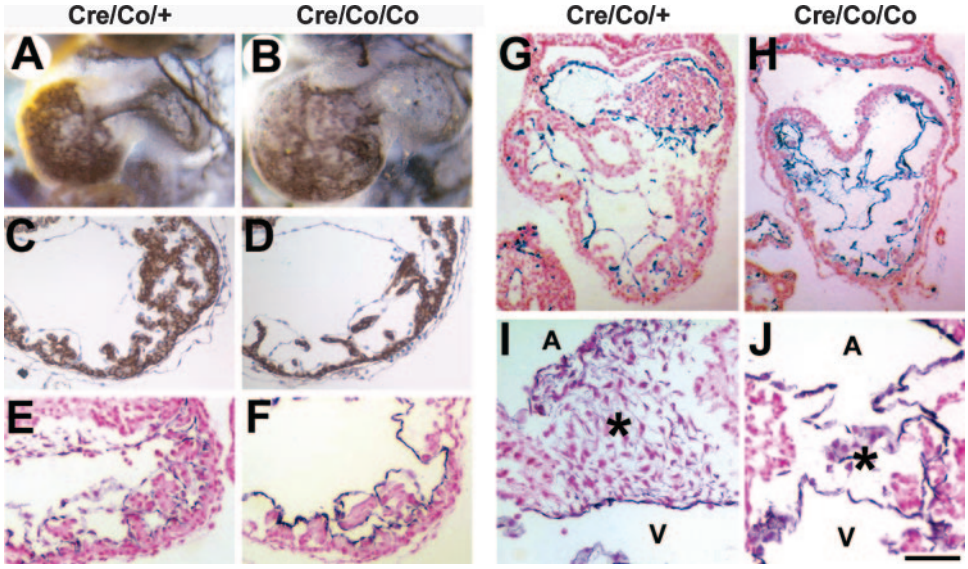

FIG. 4. Defective myocardial development and endocardial cushion formation in *Smad4$^{Co/Co}$; Tie2-Cre* embryos. (A and B) Whole-mount CD31 immunostaining of embryonic hearts at E9.5. (C and D) α-SMA immunostaining of E9.5 ventricles. (E and F) Cross sections of whole-mount CD31-stained E9.5 ventricles. Compared to the controls, the mutant embryos have enlarged hearts, dilated ventricles, and reduced trabeculae. (G and H) Cross sections of LacZ-stained hearts of *Smad4$^{Co/+}$; Tie2-Cre* and *Smad4$^{Co/Co}$; Tie2-Cre* embryos carrying a *ROSA26* allele at E9.5 show the disorganized endocardial layers of the mutant hearts. (I and J) Cross sections of a whole-mount CD31-stained atrioventricular canal at E10. The mutant embryos demonstrate significantly reduced endocardial cushion cellularity, while the cushion cells have more intensive CD31 expression than that of controls. A, atria; V, ventricles; *, endocardial cushion. Scale bar: 200 μm (A and B), 105 μm (C and D), 80 μm (E and F), 140 μm (G and H), or 55 μm (I and J).

LacZ staining of placentas carrying a *ROSA26* allele (Fig. 2M and N).

Abnormal vasculature and impaired vascular smooth muscle cells (VSMC)/preicytes development in *Smad4$^{Co/Co}$; Tie2-Cre* embryos. Globally, *Smad4$^{Co/Co}$; Tie2-Cre* embryos at E10 exhibited a coarse vascular plexus and a significant reduction of capillary vessels (Fig. 3A and B). Oversized and blind-ending vessels were easily observed in the mutant heads (Fig. 3C and D). Histologically, E9.5 mutant embryos had collapsed DAs with irregularly narrowed lumens (Fig. 3E to H and K to O), while the venous system such as the ACV showed moderately increased lumen diameters (Fig. 3H). Moreover, the parallel capillary branching from DA to somites diminished, showing nonorganized EC clusters around the DA instead (Fig. 3F). Although vessels sprouting into the neural tissue could easily be seen in E9.5 control embryos (Fig. 3G), the perineural vascular plexus of the mutant embryos was dilated and failed to invade the neuroepithelium (Fig. 3H). In addition, electron microscopy demonstrated fewer junctions with numerous intervals between adjacent mutant vascular ECs (Fig. 3I and J).

We used α-SMA immunostaining to illustrate the maturation of embryonic vessels. Transverse sections of DA revealed the development of VSMC/pericytes around the ECs of normal embryos at E9.5 (Fig. 3K and M). Nevertheless, α-SMA-positive cell around DA was hardly detected in comparable sections of the mutant embryos and failed to make close contact with adjacent ECs if any appeared (Fig. 3L and 3N). Furthermore, α-SMA expression in the somites was equivalent between the mutant and the control embryos (arrows in Fig. 3K and L), indicating that the loss of α-SMA expression was specific for VSMC/pericytes. Of note, the expression of laminin, a constituent of ECM, was unaltered in the mutant embryos, although the distribution was discontinuous due to the rupture of vascular lumens (Fig. 3O).

Defective myocardial development and endocardial cushion formation in *Smad4$^{Co/Co}$; Tie2-Cre* embryos. We further determined whether Smad4 deficiency in the endocardium affected embryonic heart development. *Smad4$^{Co/Co}$; Tie2-Cre* embryos had enlarged hearts and showed edematous pericardium (Fig. 4A and B). Dilated ventricles with reduced trabeculae of the mutant hearts were in sharp contrast to the controls (Fig. 4C to F). In some serious cases, the endocardial layer of the mutant hearts was collapsed into disorganized multiple layers and detached from myocardial trabeculae (Fig. 4G and H).

Morphogenetic process of normal endocardial cushion formation is characterized by endocardial-mesenchymal transformation with downregulating CD31 expression of cushion cells at E9.5 to 10.5 (3). However, at E9.5, atrioventricular canal endocardial cushion was totally absent in the mutant hearts (data not shown). At E10, the endocardial cushion of mutant embryos showed a dramatically decreased cellularity, and the cushion cells showed more intensively positive CD31 staining than did the controls (Fig. 4I and J). This indicated a reduced or largely missed ability of mutant endocardial cells to invade the cardiac jelly and to undergo endocardial-mesenchymal transformation.

Reduced in vitro tube formation of ECs derived from *Smad4$^{Co/Co}$; Tie2-Cre* mice. Since vessels of the mutant embryos were devoid of sprouting into placental labyrinth and neural tissue, we further investigated in vitro tube-forming capacity on Matrigel of mutant embryonic ECs to determine whether an intrinsic functional defect existed. Two strategies

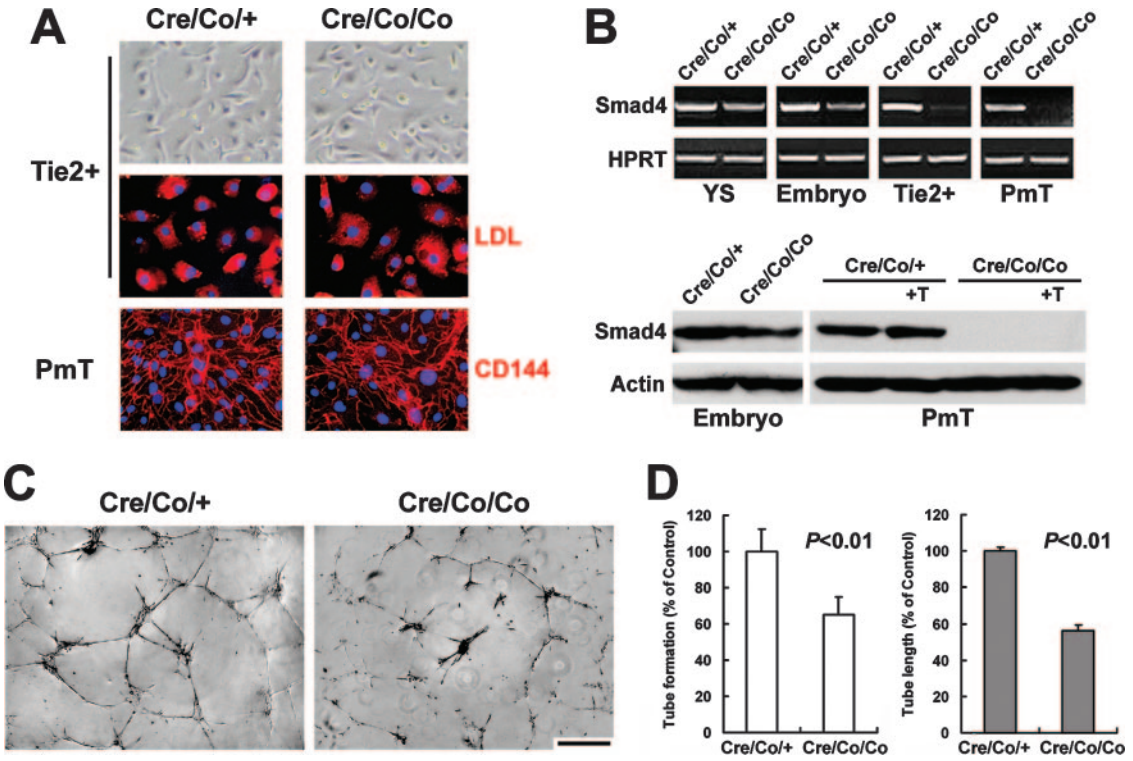

FIG. 5. Reduced in vitro tube-forming capacity of Smad4-deficient ECs. (A) Morphology and purity of isolated embryonic ECs. The upper panels show the typical cobblestone-like shape of sorted Tie2-positive cells in culture. The middle panels show >90% EC purity as verified by DiL-Ac-LDL uptake. The lower panels show the endothelial property of PmT-transformed ECs by VE-cadherin (CD144) immunostaining. (B) RT-PCR and Western blot analysis of Smad4 expression in E9.5 YS, embryos proper, sorted Tie2-positive cells, and PmT-transformed embryonic ECs is shown from left to right in the upper part of the panel. In the lower part of the panel, "+T" indicates stimulation by 10 ng of TGF-β1/ml for 20 h. Smad4 expression is reduced in the mutant embryos and absent in the mutant ECs. (C) Tube-like structures of isolated ECs on Matrigel observed after 8 h of incubation. The mutant ECs exhibit less tube formation than that of controls. (D) Quantification shows a significant 35% reduction of tube number (left) and a remarkable 44% decrease of total tube length (right) in the mutant ECs. The data are means ± the standard error of the mean. Scale bar: 27 μm (top images of panel A), 14.5 μm (middle and lower images of panel A), or 150 μm (C).

were used to obtain purified ECs from embryos. For sorted Tie2-positive cells, the purity of ECs was >90%, as evaluated by Dil-Ac-LDL incorporation (Fig. 5A). As for PmT-transformed ECs, both Dil-Ac-LDL uptake and VE-cadherin immunostaining verified their endothelial property and demonstrated unaltered expression in the Smad4-deficient ECs (Fig. 5A and data not shown). The absence of Smad4 expression in the mutant ECs was confirmed by RT-PCR and Western blot analysis (Fig. 5B). Eight hours after being plated on Matrigel, the Smad4-dificient ECs exhibited significantly attenuated capacity of forming two-dimensional tube-like structures, although they were able to change their shape and form tubes to some extent (Fig. 5C). We observed a 35% decrease in the number of tubes and a 44% reduction in the total tube length (Fig. 5D). The results strongly suggested the disrupted intrinsic function in the tube formation of Smad4-deficient ECs in vitro, corroborating the abnormal vessel sprouting and remodeling in vivo.

Altered Ang2 and Cx43 expression in Smad4-deficient ECs. To confirm whether Smad4-mediated signaling transduction was disturbed, the expression of the downstream targets was analyzed. As shown in Fig. 6A, the expression of Id1, a specific downstream target gene of ALK1-Smad1/5/8 signaling in the TGF-β pathway (12, 33), and PAI-1, which is specifically induced by ALK5-Smad2/3 (12, 33), were both clearly decreased in the mutant ECs. The results were further approved by the reporter assay using the reporters $(CAGA)_{12}$-luciferase and BRE-luciferase that are specifically responsive to Smad2/3 and Smad1, respectively (6, 13). In the control ECs, TGF-β1 stimulated the expression of both $(CAGA)_{12}$-luciferase and BRE-luciferase, whereas BMP2 activated BRE-luciferase. Nevertheless, all of the responsiveness was remarkably reduced in Smad4-deficient ECs (Fig. 6B). Unexpectedly, the expression of fibronectin 1 (Fn1) remained unchanged and even increased in the mutant ECs, although it has been considered as a direct target of ALK5 signaling (33) (Fig. 6A).

We further examined the expression of a set of genes known to be involved in blood vessel stabilization. Comparable Tie2 and PDGFB expression, but a remarkable increase of Ang2, were detected by RT-PCR and/or real-time PCR in isolated mutant ECs (Fig. 6C and D). Moreover, TGF-β1 treatment downregulated Ang2 and increased PDGFB expression, corroborating previous reports (28, 42). Nevertheless, no transcriptional change upon TGF-β1 treatment was detected in the Smad4-deficient ECs, a finding indicative of Smad4-dependent regulation of both molecules by TGF-β1 (Fig. 6D). The dramatic increase of Ang2 was also the case in the mutant embryos at both RNA and protein levels (Fig. 6E, F, and H). Flow

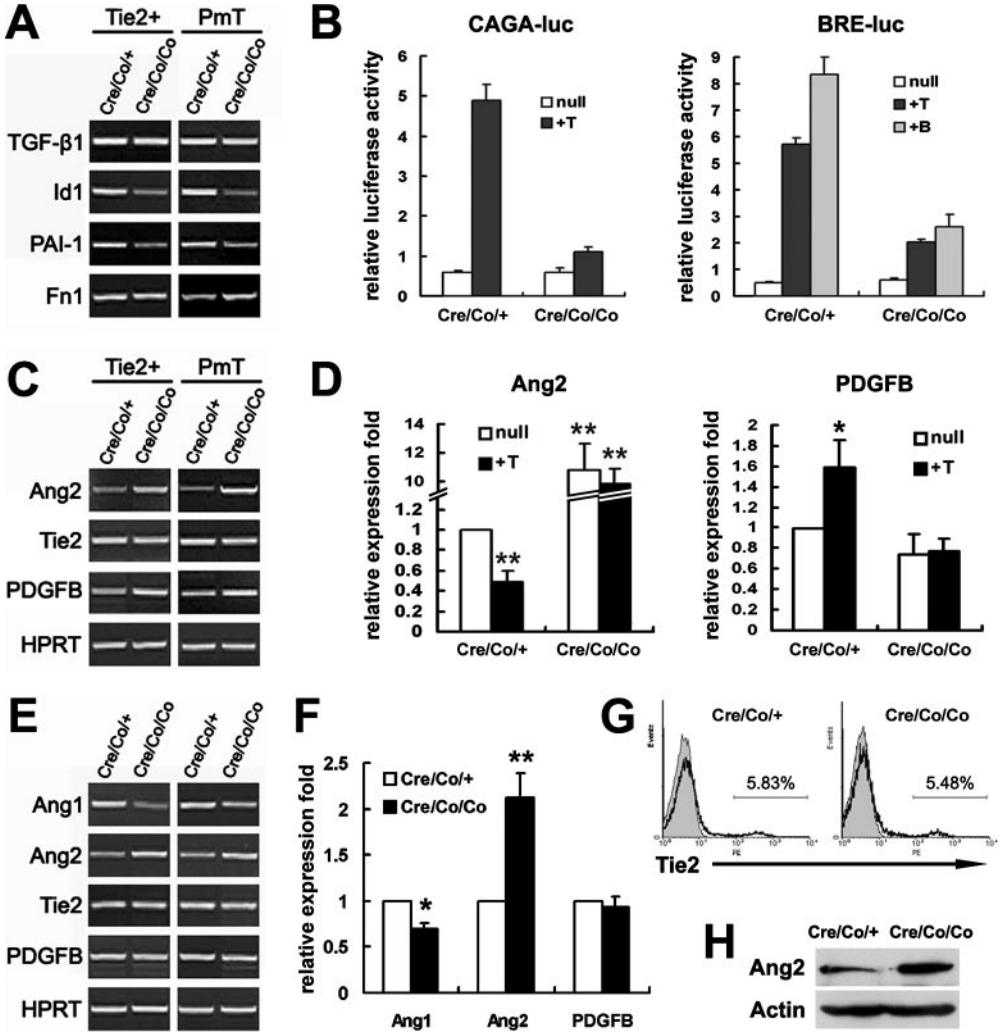

FIG. 6. Increased Ang2 expression in Smad4-deficient ECs. (A and C) RT-PCR analysis of molecular expression in isolated embryonic ECs. The data are representative of three repeats in sorted Tie2-positive cells and PmT-transformed embryonic ECs, respectively. (B) Reporter assays of PmT-transformed embryonic ECs. The cells were transfected with $(CAGA)_{12}$-luciferase or BRE-luciferase and then treated with 10 ng of TGF-β1 (+T) or 100 ng of BMP2 (+B)/ml. Inactivation of Smad4 attenuated BMP-2 and TGF-β1-stimulated luciferase activities. A representative experiment is shown. (D) Real-time PCR analysis of Ang2 and PDGFB expression using RNA extracts from PmT transformed ECs. "+T" indicates stimulation by 10 ng of TGF-β1/ml for 20 h. The mutant ECs show increased expression of Ang2 and fail to downregulate Ang2 expression upon TGF-β1 treatment. (E) RT-PCR analysis of E9.5 whole-embryo RNA extracts. The data are two representatives of four independent experiments. (F) Real-time PCR analysis of Ang1, Ang2, and PDGFB expression using E9.5 whole-embryo RNA extracts. (G) Flow cytometric analysis of Tie2 expression in whole embryos. A representative experiment is shown. (H) Western blot analysis of E9.5 whole embryos demonstrates increased Ang2 expression in the mutants. The data are expressed as means ± the standard error of the mean. *, $P < 0.05$; **, $P < 0.01$ (significantly different from the untreated controls in panels D and F).

cytometric analysis further approved the equivalent embryonic Tie2 expression at protein level (Fig. 6G). In addition, being mesenchyme derived and important for stabilizing vessel walls (4), Ang1 showed modestly reduced expression in the mutant embryos (Fig. 6E and F).

Given that Cx43-mediated gap junctional communication between endothelial and mesenchymal cells is crucial for mural cell differentiation (15), we examined the expression of Cx43, which is also involved in mouse vascular development (25). Cx43 expression was reduced in cultured Smad4-deficient ECs (Fig. 7A). Upon TGF-β1 treatment, Cx43 expression was upregulated in the control ECs as previously reported (21). However, we demonstrated at both RNA and protein levels that the expression of Cx43 hardly increased but rather decreased in the mutant ECs when treated with TGF-β1 (Fig. 7B and C). Importantly, a remarkable reduction of Cx43 expression was detected in the vascular ECs of E9.5 mutant embryos in vivo (Fig. 7D).

DISCUSSION

Targeted disruption of *Smad4* in mice results in early embryonic lethality with multiple defects on epiblast proliferation, egg cylinder formation, and mesoderm induction. Thus, a systematic and precise analysis of vascular development is unavailable (50). Here, disruption of Smad4 specifically in ECs

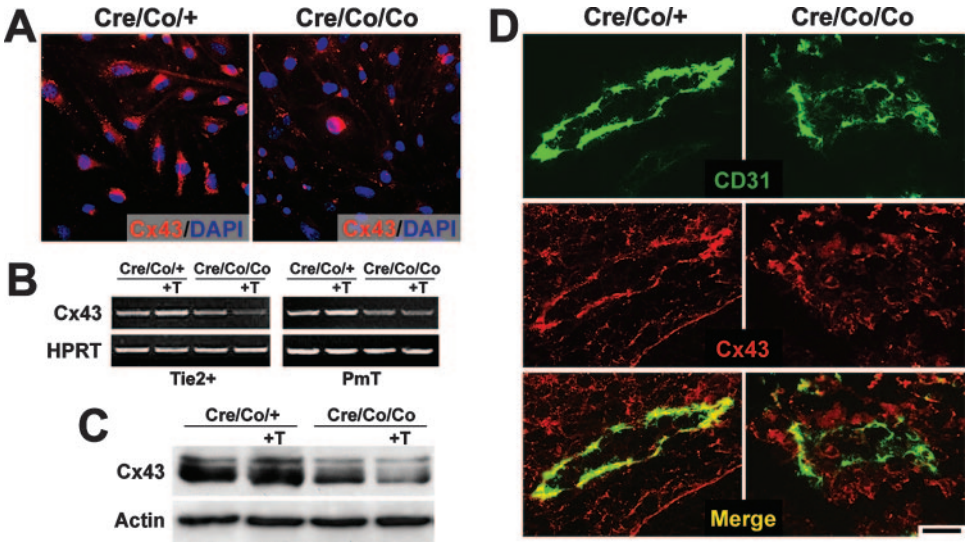

FIG. 7. Reduced expression of Cx43 in Smad4-deficient ECs. (A) Immunofluorescence labeling of Cx43 in PmT-transformed ECs. The Smad4-deficient ECs demonstrate notably reduced expression. (B) Representative RT-PCR analysis of Cx43 expression using RNA extracts from isolated Tie2-positive cells (left side) and PmT-transformed ECs (right side). (C) Western blotting analysis of Cx43 expression in PmT-transformed ECs. "+T" indicates stimulated by 10 ng of TGF-β1/ml for 20 h. The mutant ECs fail to upregulate the expression of Cx43 upon treatment of TGF-β1. (D) Cx43 Immunofluorescence staining of E9.5 DAs shows reduced expression in the mutant vascular ECs in vivo. Scale bar: 12 μm (A) or 25 μm (D).

led to embryonic lethality by E10.5 due to multiple cardiovascular defects, demonstrating a pivotal role of endothelial Smad4 in vascular remodeling and stabilization.

We revealed an indispensable function of endothelial Smad4 in angiogenesis. Smad4-deficient ECs were able to assemble into a primary vascular plexus, suggesting that vasculogenesis was intact in the mutant mice. However, the Smad4-deficient primary vessels failed to undergo remodeling and efficient spouting in vivo, indicating that angiogenesis is definitely abnormal in *Smad4* mutants. The angiogenesis defects largely mimicked the phenotypes of the loss-of-function mutant mice in which a variety of other members of TGF-β signaling pathway were globally disrupted (7, 22, 24, 31, 32, 48), a finding indicative of an essential cell-autonomous role of Smad4 signaling in ECs during vascular development. Most recently, a conditional *Smad4* knockout mouse driven by a *Flk1* promoter has been reported to manifest similar angiogenesis defects in the YS, whereas the influence on embryos proper is not known (34). Since Flk1 expression marks a broad spectrum of mesodermal progenitors besides ECs in the early mouse embryos (9, 30), it may further emphasize the endothelium as the predominant cell type responsible for Smad4-related vascular defect. Actually, the *Smad4*$^{Co/Co}$*; Tie2-Cre* embryos also exhibited some distinct phenotypes. The DAs of *Smad4*$^{Co/Co}$*; Tie2-Cre* embryos displayed irregularly narrowed lumen and were ruptured. It was much more outstanding than the changes in veins with moderate dilatation only. In the *TGF-β1*, *TβR2*, *ALK5*, and *endoglin* knockout embryos, the lumen size and shape of the DAs are comparable to those found in wild-type mice (7, 22, 24, 32), whereas in the *ALK1* and *Smad5* knockout mice, the blood vessels are greatly dilated at E9.5 (31, 48). In contrast to a recent study showing that the Tie2 promoter is much more active in the arterial system than in the venous system (1), the Tie2 promoter in combination with the enhancer fragment we used in the present study ensured the equivalent Cre expression throughout the cardiovascular system (19, 36). Since *Smad4* was authentically deleted in all vascular ECs (Fig. 1G and 5B), the phenotypic discrepancy between the DA and the venous system in the mutant E9.5 embryos presumably resulted from distinct roles rather than different knockout efficiency of Smad4 in arterial versus venous vessels. Notably, ALK1 is predominantly expressed in arteries over veins (12, 38), suggesting that Smad4-mediated ALK1 signals might play somewhat more significant roles in arterial ECs. It requires further clarification as to how Smad4 deficiency in ECs exerts different influences on the structure of arterial versus venous vessels.

Disrupted remodeling of embryonic vasculature in *Smad4* mutants was largely due to intrinsic functional defects of *Smad4* mutant ECs. Gain-of-function studies show that, whereas ALK1 via Smad1/5 stimulates EC migration and tube formation (12, 47), ALK5 via Smad2/3 inhibits EC migration and tube formation (12, 33, 47). Hence, TGF-β exerts bifunctional effects on EC via a fine balance between ALK5 and ALK1 signaling (12). Moreover, the opposite effects on EC migration mediated by ALK1 and ALK5 are Smad4 dependent (12). Nevertheless, ALK5-deficient ECs demonstrate intact tube-forming properties in vitro (22), and up-to-date, few evidence has shown EC defect in tube formation in vitro by loss-of-function studies on TGF-β signaling components. Here, we demonstrated the intrinsic defect in tube formation of Smad4-defecient ECs, which was a little unexpected since exogenous TGF-β also inhibits the formation of tube-like structures of ECs on Matrigel (33). The defect presumably resulted from a disturbed balance between the ALK1 and ALK5 pathways. Except for TGF-β1, the significance of BMP signaling in EC behavior has been elucidated in vitro and in vivo (34, 46). The Smad4-deficent ECs remarkably reduced the

responsiveness to BMP2 and manifested a significant decrease in Id1 expression, which is a direct target of both TGF-β1–ALK1 and BMP signaling. Therefore, disruption of Smad4-mediated BMP signaling may synergistically account for the attenuated tube-forming capacity of Smad4-deficient ECs and the vascular abnormalities of mutant embryos.

TGF-β1 is thought to have a direct stimulatory effect on the synthesis and deposition of ECM components by ECs, inducing Fn and laminin production through ALK5 signaling (33, 45). Unexpectedly, the expression of Fn and laminin demonstrated hardly reduced in the Smad4-deficient ECs, although ALK5-Smad2/3 signaling was indeed attenuated. These results suggested that Smad4 is not required for the expression of some ECM components in developing ECs. Supportively, TGF-β can modulate the expression of Fn gene in a Smad4-independent manner in some non-EC cell types (17, 44).

Deletion of *Smad4* exclusively in ECs might provide abnormal signals for impaired cellular interaction between endothelial and surrounding cells. Angiopoietins promote vessel stability by activating (Ang1) or antagonizing (Ang2) signaling via the Tie2 receptor (4). The disturbed balance between Ang1 and Ang2, especially the remarkable increase of Ang2, in the *Smad4$^{Co/Co}$; Tie2-Cre* embryos was inclined to destroy the vessel stability. In mid-gestational mouse embryos, Ang2 expression was abundant in the DA and major aortic branches, specifically in the VSMC beneath the vessel endothelium (10, 27). However, its expression was induced within the ECs of small vessels at sites of vascular remodeling (8, 10). Although increased expression of Ang2 in the mutant embryos could be a secondary response to the remodeling defects in vivo, most importantly, we revealed that lack of Smad4 in ECs lead to a cell-autonomous increase of endothelial Ang2 expression. In vitro, exogenous Ang2 destabilizes quiescent endothelium and leads to prominent EC detachment in a three-dimensional coculture model (35). It is noteworthy that some of the vascular defects in *Smad4$^{Co/Co}$; Tie2-Cre* embryos were highly reminiscent of those observed in Ang2 overexpression transgenic mice, particularly the notable vessel discontinuities and the apparent collapse of endocardium (27). Interestingly, although neither ALK1 nor ALK5 alone modulates Ang2 expression (33, 47), TGF-β1 downregulated Ang2 expression in a Smad4-dependent manner, implying somewhat complicated regulatory mechanisms. It is possible that Smad4 signaling influences EC behavior partially through modulating angiopoietin signals or that there exists a cross talking between the two pathways, but further investigation is required.

By virtue, dissociation of ECs away from the surrounding cells in *Smad4$^{Co/Co}$; Tie2-Cre* embryos was universal and prominent. Here we highlighted a candidate molecule, Cx43, as a structure basis for the intercellular disassociation. The decreased expression of Cx43 in the Smad4-deficient ECs was most likely cell autonomous because the results shown both in situ and in the cultured ECs were coincident. Interestingly, the responsiveness of Cx43 expression to TGF-β1 treatment in the mutant ECs was converse to that in the controls, suggesting that Smad4-independent regulation of endothelial Cx43 expression by TGF-β1 might exist. Functionally, Cx43-mediated gap junctional communication between endothelial and mesenchymal cells is crucial for latent TGF-β1 activation and subsequent endothelium-induced mural cell differentiation (15). Hence, it is conceivable that cell contact-dependent activation of TGF-β1 may be largely disturbed in the *Smad4* mutant embryos (2), although TGF-β1 transcription remained unchanged. Supportively, it is suggested that disruption of TGF-β signaling exclusively in vascular ECs results in reduced availability of TGF-β1 protein to adjacent cells, whereas the transcription of TGF-β1 is unaltered (5). Thus, cell-autonomous downregulation of Cx43 in the Smad4-deficient ECs, which probably results in impaired gap junctional communication between ECs and surrounding cells, might contribute to the impaired VSMC recruitment and destabilized vasculature in the mutant embryos.

In summary, we have provided direct functional evidences that Smad4 activity in the developing ECs is essential for embryonic cardiovascular development. Further studies investigating the detailed molecular basis of Smad4 signaling in ECs, possibly including angiopoietins and gap junction molecules, are required to understand definitely the role of Smad4 signaling in vascular remodeling and integrity in embryonic development, as well as in adult tissues and tumor models.

ACKNOWLEDGMENTS

This study was supported by the National Key Basic Research Program of China (2005CB522506, 2005CB522705, and 2006CB943501), the National Natural Science Foundation of China (30671077), the National Hi-Tech R&D Program (2006AA02Z168), the National Science and Technology Supporting Program (2006BAI23B01-03), and Beijing Science Projects (10006303041231).

We thank Chuxia Deng at the National Institutes of Health (NIH) for the *Smad4* conditional gene targeting mouse, Hua Gu at the NIH for Cre plasmid, and Xiang Gao at Nanjing University for the mouse strains. We also thank Jincai Luo at Peking University for instruction on selective transformation of ECs and related retrovirus and cell lines, and we thank Yeguang Chen at Tsinghua University for reporters.

REFERENCES

1. **Anghelina, M., L. Moldovan, and N. I. Moldovan.** 2005. Preferential activity of Tie2 promoter in arteriolar endothelium. J. Cell Mol. Med. **9:**113–121.
2. **Antonelli-Orlidge, A., K. B. Saunders, S. R. Smith, and P. A. D'Amore.** 1989. An activated form of transforming growth factor beta is produced by cocultures of endothelial cells and pericytes. Proc. Natl. Acad. Sci. USA **86:**4544–4548.
3. **Armstrong, E. J., and J. Bischoff.** 2004. Heart valve development: endothelial cell signaling and differentiation. Circ. Res. **95:**459–470.
4. **Armulik, A., A. Abramsson, and C. Betsholtz.** 2005. Endothelial/pericyte interactions. Circ. Res. **97:**512–523.
5. **Carvalho, R. L., L. Jonker, M. J. Goumans, J. Larsson, P. Bouwman, S. Karlsson, P. T. Dijke, H. M. Arthur, and C. L. Mummery.** 2004. Defective paracrine signaling by TGFβ in yolk sac vasculature of endoglin mutant mice: a paradigm for hereditary haemorrhagic telangiectasia. Development **131:**6237–6247.
6. **Dennler, S., S. Itoh, D. Vivien, P. ten Dijke, S. Huet, and J. M. Gauthier.** 1998. Direct binding of Smad3 and Smad4 to critical TGFβ-inducible elements in the promoter of human plasminogen activator inhibitor-type 1 gene. EMBO J. **17:**3091–3100.
7. **Dickson, M. C., J. S. Martin, F. M. Cousins, A. B. Kulkarni, S. Karlsson, and R. J. Akhurst.** 1995. Defective hematopoiesis and vasculogenesis in transforming growth factor-β1 knockout mice. Development **121:**1845–1854.
8. **Eklund, L., and B. R. Olsen.** 2006. Tie receptors and their angiopoietin ligands are context-dependent regulators of vascular remodeling. Exp. Cell Res. **312:**630–641.
9. **Ema, M., S. Takahashi, and J. Rossant.** 2006. Deletion of the selection cassette, but not *cis*-acting elements, in targeted Flk1-lacZ allele reveals Flk1 expression in multipotent mesodermal progenitors. Blood **107:**111–117.
10. **Gale, N. W., G. Thurston, S. F. Hackett, R. Renard, Q. Wang, J. McClain, C. Martin, C. Witte, M. H. Witte, D. Jackson, C. Suri, P. A. Campochiaro, S. J. Wiegand, and G. D. Yancopoulos.** 2002. Angiopoietin-2 is required for postnatal angiogenesis and lymphatic patterning, and only the latter role is rescued by Angiopoietin-1. Dev. Cell **3:**411–423.
11. **Gallione, C. J., G. M. Repetto, E. Legius, A. K. Rustgi, S. L. Schelley, S. Tejpar, G. Mitchell, E. Drouin, C. J. Westermann, and D. A. Marchuk.** 2004.

A combined syndrome of juvenile polyposis and hereditary haemorrhagic telangiectasia associated with mutations in MADH4 (SMAD4). Lancet **363:** 852–859.
12. **Goumans, M. J., G. Valdimarsdottir, S. Itoh, A. Rosendahl, P. Sideras, and P. ten Dijke.** 2002. Balancing the activation state of the endothelium via two distinct TGF-β type I receptors. EMBO J. **21:**1743–1753.
13. **Hata, A., J. Seoane, G. Lagna, E. Montalvo, A. Hemmati-Brivanlou, and J. Massague.** 2000. OAZ uses distinct DNA- and protein-binding zinc fingers in separate BMP-Smad and Olf signaling pathways. Cell **100:**229–240.
14. **Hatzopoulos, A. K., J. Folkman, E. Vasile, G. K. Eiselen, and R. D. Rosenberg.** 1998. Isolation and characterization of endothelial progenitor cells from mouse embryos. Development **125:**1457–1468.
15. **Hirschi, K. K., J. M. Burt, K. D. Hirschi, and C. Dai.** 2003. Gap junction communication mediates transforming growth factor-beta activation and endothelial-induced mural cell differentiation. Circ. Res. **93:**429–437.
16. **Hirschi, K. K., S. A. Rohovsky, and P. A. D'Amore.** 1998. PDGF, TGF-beta, and heterotypic cell-cell interactions mediate endothelial cell-induced recruitment of 10T1/2 cells and their differentiation to a smooth muscle fate. J. Cell Biol. **141:**805–814.
17. **Hocevar, B. A., T. L. Brown, and P. H. Howe.** 1999. TGF-beta induces fibronectin synthesis through a c-Jun N-terminal kinase-dependent, Smad4-independent pathway. EMBO J. **18:**1345–1356.
18. **Johnson, D. W., J. N. Berg, M. A. Baldwin, C. J. Gallione, I. Marondel, S. J. Yoon, T. T. Stenzel, M. Speer, M. A. Pericak-Vance, A. Diamond, A. E. Guttmacher, C. E. Jackson, L. Attisano, R. Kucherlapati, M. E. Porteous, and D. A. Marchuk.** 1996. Mutations in the activin receptor-like kinase 1 gene in hereditary haemorrhagic telangiectasia type 2. Nat. Genet. **13:**189–195.
19. **Kisanuki, Y. Y., R. E. Hammer, J. Miyazaki, S. C. Williams, J. A. Richardson, and M. Yanagisawa.** 2001. Tie2-Cre transgenic mice: a new model for endothelial cell-lineage analysis in vivo. Dev. Biol. **230:**230–242.
20. **Kwak, B. R., M. S. Pepper, D. B. Gros, and P. Meda.** 2001. Inhibition of endothelial wound repair by dominant negative connexin inhibitors. Mol. Biol. Cell **12:**831–845.
21. **Larson, D. M., T. G. Christensen, G. D. Sagar, and E. C. Beyer.** 2001. TGF-beta1 induces an accumulation of connexin43 in a lysosomal compartment in endothelial cells. Endothelium **8:**255–260.
22. **Larsson, J., M. J. Goumans, L. J. Sjostrand, M. A. van Rooijen, D. Ward, P. Leveen, X. Xu, P. ten Dijke, C. L. Mummery, and S. Karlsson.** 2001. Abnormal angiogenesis but intact hematopoietic potential in TGF-β type I receptor-deficient mice. EMBO J. **20:**1663–1673.
23. **Lebrin, F., M. Deckers, P. Bertolino, and P. Ten Dijke.** 2005. TGF-beta receptor function in the endothelium. Cardiovasc. Res. **65:**599–608.
24. **Li, D. Y., L. K. Sorensen, B. S. Brooke, L. D. Urness, E. C. Davis, D. G. Taylor, B. B. Boak, and D. P. Wendel.** 1999. Defective angiogenesis in mice lacking endoglin. Science **284:**1534–1537.
25. **Li, W. E., K. Waldo, K. L. Linask, T. Chen, A. Wessels, M. S. Parmacek, M. L. Kirby, and C. W. Lo.** 2002. An essential role for connexin43 gap junctions in mouse coronary artery development. Development **129:**2031–2042.
26. **Li, W. L., X. Cheng, X. H. Tan, J. S. Zhang, Y. S. Sun, L. Chen, and X. Yang.** 2005. Endothelial cell-specific expression of Cre recombinase in transgenic mice. Yi Chuan Xue Bao **32:**909–915.
27. **Maisonpierre, P. C., C. Suri, P. F. Jones, S. Bartunkova, S. J. Wiegand, C. Radziejewski, D. Compton, J. McClain, T. H. Aldrich, N. Papadopoulos, T. J. Daly, S. Davis, T. N. Sato, and G. D. Yancopoulos.** 1997. Angiopoietin-2, a natural antagonist for Tie2 that disrupts in vivo angiogenesis. Science **277:**55–60.
28. **Mandriota, S. J., and M. S. Pepper.** 1998. Regulation of angiopoietin-2 mRNA levels in bovine microvascular endothelial cells by cytokines and hypoxia. Circ. Res. **83:**852–859.
29. **McAllister, K. A., K. M. Grogg, D. W. Johnson, C. J. Gallione, M. A. Baldwin, C. E. Jackson, E. A. Helmbold, D. S. Markel, W. C. McKinnon, J. Murrell, et al.** 1994. Endoglin, a TGF-β binding protein of endothelial cells, is the gene for hereditary haemorrhagic telangiectasia type 1. Nat. Genet. **8:**345–351.
30. **Motoike, T., D. W. Markham, J. Rossant, and T. N. Sato.** 2003. Evidence for novel fate of Flk1+ progenitor: contribution to muscle lineage. Genesis **35:**153–159.
31. **Oh, S. P., T. Seki, K. A. Goss, T. Imamura, Y. Yi, P. K. Donahoe, L. Li, K. Miyazono, P. ten Dijke, S. Kim, and E. Li.** 2000. Activin receptor-like kinase 1 modulates transforming growth factor-β1 signaling in the regulation of angiogenesis. Proc. Natl. Acad. Sci. USA **97:**2626–2631.
32. **Oshima, M., H. Oshima, and M. M. Taketo.** 1996. TGF-beta receptor type II deficiency results in defects of yolk sac hematopoiesis and vasculogenesis. Dev. Biol. **179:**297–302.
33. **Ota, T., M. Fujii, T. Sugizaki, M. Ishii, K. Miyazawa, H. Aburatani, and K. Miyazono.** 2002. Targets of transcriptional regulation by two distinct type I receptors for transforming growth factor-beta in human umbilical vein endothelial cells. J. Cell Physiol. **193:**299–318.
34. **Park, C., K. Lavine, Y. Mishina, C. X. Deng, D. M. Ornitz, and K. Choi.** 2006. Bone morphogenetic protein receptor 1A signaling is dispensable for hematopoietic development but essential for vessel and atrioventricular endocardial cushion formation. Development **133:**3473–3484.
35. **Scharpfenecker, M., U. Fiedler, Y. Reiss, and H. G. Augustin.** 2005. The Tie-2 ligand angiopoietin-2 destabilizes quiescent endothelium through an internal autocrine loop mechanism. J. Cell Sci. **118:**771–780.
36. **Schlaeger, T. M., S. Bartunkova, J. A. Lawitts, G. Teichmann, W. Risau, U. Deutsch, and T. N. Sato.** 1997. Uniform vascular-endothelial-cell-specific gene expression in both embryonic and adult transgenic mice. Proc. Natl. Acad. Sci. USA **94:**3058–3063.
37. **Schwarte-Waldhoff, I., O. V. Volpert, N. P. Bouck, B. Sipos, S. A. Hahn, S. Klein-Scory, J. Luttges, G. Kloppel, U. Graeven, C. Eilert-Micus, A. Hintelmann, and W. Schmiegel.** 2000. Smad4/DPC4-mediated tumor suppression through suppression of angiogenesis. Proc. Natl. Acad. Sci. USA **97:**9624–9629.
38. **Seki, T., J. Yun, and S. P. Oh.** 2003. Arterial endothelium-specific activin receptor-like kinase 1 expression suggests its role in arterialization and vascular remodeling. Circ. Res. **93:**682–689.
39. **Soriano, P.** 1999. Generalized lacZ expression with the ROSA26 Cre reporter strain. Nat. Genet. **21:**70–71.
40. **Sun, Y., J. Zhou, X. Liao, Y. Lu, C. Deng, P. Huang, Q. Chen, and X. Yang.** 2005. Disruption of Smad5 gene induces mitochondria-dependent apoptosis in cardiomyocytes. Exp. Cell Res. **306:**85–93.
41. **Tang, N., F. Mack, V. H. Haase, M. C. Simon, and R. S. Johnson.** 2006. pVHL function is essential for endothelial extracellular matrix deposition. Mol. Cell. Biol. **26:**2519–2530.
42. **Taylor, L. M., and L. M. Khachigian.** 2000. Induction of platelet-derived growth factor B-chain expression by transforming growth factor-beta involves transactivation by Smads. J. Biol. Chem. **275:**16709–16716.
43. **ten Dijke, P., and C. S. Hill.** 2004. New insights into TGF-β-Smad signaling. Trends Biochem. Sci. **29:**265–273.
44. **Tsuchida, K., Y. Zhu, S. Siva, S. R. Dunn, and K. Sharma.** 2003. Role of Smad4 on TGF-β-induced extracellular matrix stimulation in mesangial cells. Kidney Int. **63:**2000–2009.
45. **Usui, T., M. Takase, Y. Kaji, K. Suzuki, K. Ishida, T. Tsuru, K. Miyata, M. Kawabata, and H. Yamashita.** 1998. Extracellular matrix production regulation by TGF-β in corneal endothelial cells. Investig. Ophthalmol. Vis. Sci. **39:**1981–1989.
46. **Valdimarsdottir, G., M. J. Goumans, A. Rosendahl, M. Brugman, S. Itoh, F. Lebrin, P. Sideras, and P. ten Dijke.** 2002. Stimulation of Id1 expression by bone morphogenetic protein is sufficient and necessary for bone morphogenetic protein-induced activation of endothelial cells. Circulation **106:**2263–2270.
47. **Wu, X., J. Ma, J. D. Han, N. Wang, and Y. G. Chen.** 2006. Distinct regulation of gene expression in human endothelial cells by TGF-β and its receptors. Microvasc. Res. **71:**12–19.
48. **Yang, X., L. H. Castilla, X. Xu, C. Li, J. Gotay, M. Weinstein, P. P. Liu, and C. X. Deng.** 1999. Angiogenesis defects and mesenchymal apoptosis in mice lacking SMAD5. Development **126:**1571–1580.
49. **Yang, X., C. Li, P. L. Herrera, and C. X. Deng.** 2002. Generation of Smad4/Dpc4 conditional knockout mice. Genesis **32:**80–81.
50. **Yang, X., C. Li, X. Xu, and C. Deng.** 1998. The tumor suppressor SMAD4/DPC4 is essential for epiblast proliferation and mesoderm induction in mice. Proc. Natl. Acad. Sci. USA **95:**3667–3672.